SolarPACES 2022, 28th International Conference on Concentrating Solar Power and Chemical Energy Systems
Solar Fuels and Chemical Commodities
https://doi.org/10.52825/solarpaces.v1i.684

Published: 09 Feb. 2024

Computational Fluid Dynamics Modeling of Solar Thermal Dry Reforming of Methane in a Parabolic Trough

Clifford K. Ho[1] and Christopher R. Riley[2]

[1] Sandia National Laboratories, Climate Change Security Center, Albuquerque, NM, USA
ckho@sandia.gov

[2] Sandia National Laboratories, Electronic, Optical, and Nano Materials, Albuquerque, NM, USA
crriley@sandia.gov

Abstract. Computational fluid dynamics simulations of solar-thermal dry reforming of methane using a parabolic trough configuration were performed. Parametric simulations of different combinations of gas flow rate, receiver tube emissivity, and geometric concentration ratio were conducted to determine configurations that could achieve the required catalyst temperatures of at least 700 °C to achieve high conversion of CH_4 and CO_2 to H_2 and CO. Results showed that the concentration ratio of the parabolic trough collector had to be increased from ~70 to ~120 and the receiver-tube emissivity had to be reduced to ~0.2 to achieve bulk average catalyst temperatures of greater than 700 °C. Lower gas flow rates also reduced enthalpic heat losses and increased catalyst temperatures.

Keywords: Dry reforming, Methane, Parabolic Trough

1 Introduction

Flaring (or combustion) of natural gas occurs during production and extraction of oil from the subsurface. If sufficient natural gas exists, it may be economical to extract the gas as a value-added feedstock along with the oil, if it can be collected and processed cost-effectively. Due to the expense of current techniques used to capture or recover the natural gas, the gas is often burned for safety, economic, or operational reasons. Currently, the U.S. flares ~6 – 8 billion cubic meters (~200 – 300 billion cubic feet) of extracted natural gas each year [1], amounting to over $700 million in lost revenue annually. Globally, ~140 billion cubic meters (~5 trillion cubic feet) of natural gas were flared in 2020, nearly equivalent to the amount of natural gas demand in Central and South America [2]. Global flaring results in ~300 – 600 million metric tons of CO_2 being emitted into the atmosphere annually [2, 3]. Russia, Iraq, Iran, United States, and Algeria were responsible for over half of all flaring volumes [2].

Sandia National Laboratories is developing a solar-thermal system to process natural gas currently wasted at extraction sites through routine flaring. Our system facilitates the dry reforming of methane (DRM) reaction with compositionally complex, multi-cationic aluminate spinel catalysts. These catalysts simultaneously achieve the thermal stability, product selectivity, and catalytic activity necessary to efficiently convert methane and carbon dioxide to hydrogen and carbon monoxide, valuable feedstocks for hydrocarbon fuels. Carbon dioxide co-reactant is already widely injected into oil and natural gas reserves through enhanced oil recovery and enhanced gas recovery processes. Concentrated sunlight from a parabolic trough collector is

used to provide fossil-free heat for the highly endothermic reaction. Our system uses a trough-type collector to concentrate and direct sunlight onto a specially designed tube reactor to heat the contained catalyst to relevant reaction temperatures (700 – 800 °C) (Figure 1). An inert porous material (e.g., sand, gravel, SiC beads) is packed upstream of the catalyst within the receiver tube to preheat the flowing gas to higher temperatures prior to reaching the catalyst.

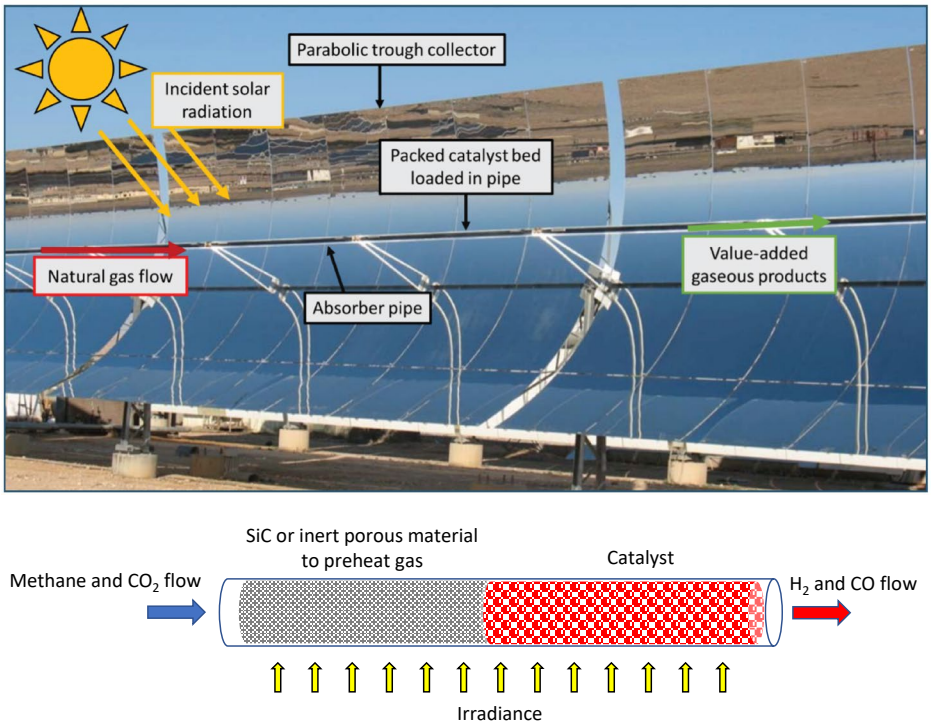

Figure 1. Top: schematic of a field-deployable parabolic trough concentrating solar collector with housed packed catalyst bed. Bottom: trough receiver tube packed with porous media and catalyst.

This system incorporates several potential improvements relative to previous solar-thermal DRM systems employing either point-focus systems or membrane separation in troughs [4-6]. Improvements include the use of a preheating material, parabolic trough with dimensions amenable to mobile transport, and an improved multi-cationic catalyst. Although industry does not currently implement this reaction, DRM can be performed in decentralized facilities at much milder temperatures and pressures than steam reforming conventionally performed at large, centralized chemical plants, which enables the proposed DRM design to be used and mobilized at flaring sites at lower costs.

The focus of this paper is on computational fluid dynamics (CFD) modeling to determine the design parameters and trough configurations that will enable heating the CO_2 and CH_4 gas and catalyst to sufficient temperatures for the catalytic reactions to occur above 700 °C.

2 Modeling Approach

A CFD model of the proposed parabolic-trough DRM reactor was developed using Solidworks Flow Simulation, which solves the conservation of mass, momentum, energy, and species equations using a discrete numerical finite-volume approach and a k-ε turbulence model with modified wall functions [7]. The 8-m-long parabolic trough assembly was modeled after the LS-2 design with a 5-m aperture and 1.5 m focal length. The 8-m receiver tube was packed on the upstream end (4 m) with a porous media (assumed porosity = 0.5, solid density = 2630 kg/m^3, specific heat = 775 J/kg-K, thermal conductivity = 2.79 W/m-K) to serve as a preheater

for the equimolar concentration of CO_2 and CH_4 flowing into the receiver tube. On the downstream end, the tube was packed with catalyst (porosity = 0.5, solid density = 4500 kg/m^3, specific heat = 550 J/kg-K, thermal conductivity = 70 W/m-K) that has a heat of reaction of 259 kJ/mol, normalized to a mole of each reactant gas. The kinetics of reaction are neglected, and the product of the heat of reaction and molar flow rate of each reactant gas are used to determine the thermal power (heat sink) required for the reaction, which is assumed to be complete within the prescribed length of the catalyst bed. The solid/fluid heat-transfer coefficients in both the porous preheat material and the catalyst were assumed to be velocity dependent and taken from Ho and Gerstle [8] and Wu and Hwang [9]. The solar irradiance on the parabolic-trough collector was assumed to be 1000 W/m^2 with a normal incidence angle and 94% collector reflectivity. Both radiative (α = ε = 0.9) and convective heat loss from the receiver were simulated under quiescent conditions. A grid convergence study was performed by systematically increasing the mesh resolution (from ~60K to ~1M cells) to determine when the key simulated metric (bulk catalyst gas temperature) no longer changed with mesh size. A mesh with ~540K cells was found to be suitable for the current simulations (see Figure 2). A parametric study was performed to evaluate the combination of gas flow rate, concentration ratio, and receiver emissivity that yielded catalyst temperatures greater than the required reaction temperature of 700 °C.

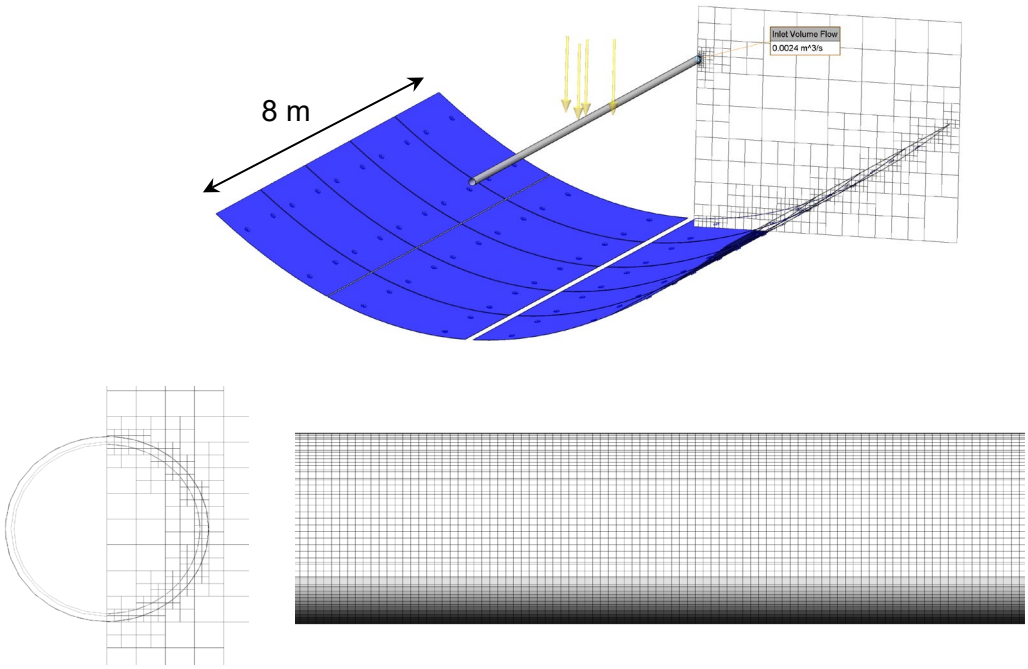

Figure 2. Model domain (top) and sample mesh (bottom) used in this study.

3 Modeling Results

3.1 Optical Modeling

Figure 3 shows the results of the solar ray tracing of the LS-2 parabolic trough using a half-symmetry model in Solidworks Flow Simulation. The geometry of the mirror facets was modeled from measurements of an LS-2 parabolic trough at Sandia [10], yielding an optical intercept factor of 0.97 – 0.98 (i.e., 97 – 98% of the solar radiation leaving the collector is intercepted by the receiver tube). Based on the position of the receiver tube relative to the collector, the majority of the incident solar radiation strikes the lower half of the receiver tube. Heat from the incident solar radiation is then conducted through the stainless-steel receiver tube to the porous media or catalyst inside. No quartz glass envelope tube, which is often used to minimize convective heat losses in parabolic trough concentrating solar power plants, is modeled.

The geometric concentration ratio of the modelled LS-2 parabolic trough collector with a 5-m aperture and 70-mm receiver tube was ~70 (i.e., the solar flux (W/m^2) on the receiver tube was ~70 times the solar irradiance from the sun). For the parametric analysis, the concentration ratio was increased to ~120, which represents an increase in the trough collector aperture from 5 m to just over ~8 m, to achieve the desired catalyst temperatures. The additional costs (and potential reduced optical accuracy) of a larger parabolic trough need to be considered in future technoeconomic analyses.

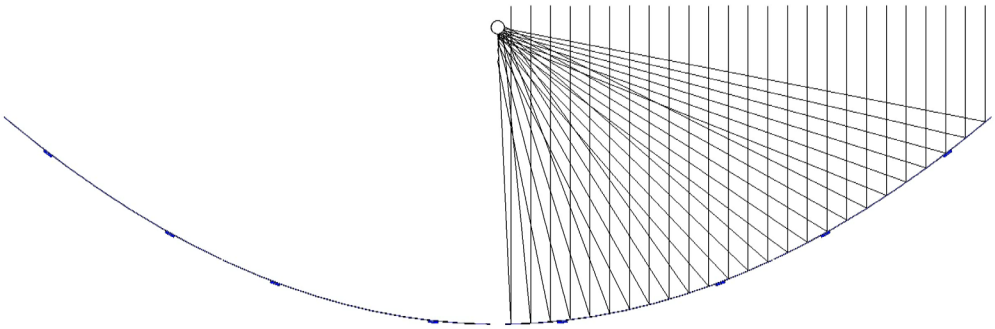

Figure 3. Optical modeling of LS-2 parabolic trough and receiver tube used for DRM simulations. Half-symmetry is employed in the model.

3.2 Heat-Transfer Modeling

CFD simulations using a 10 ft^3/min (0.0047 m^3/s) gas flow rate and receiver-tube emissivity of 0.9, and equal gravel and catalyst lengths of 4 m showed that the gas temperatures increased to just over 500 °C at the end of the porous preheat section (midway) and then began to cool as a result of the large endothermic enthalpy of reaction enabled by the catalyst. To yield desired bulk average catalyst temperatures of 700 °C, the geometric concentration ratio had to be increased from ~70 to ~120 (i.e., trough aperture increased from 5 m to just over 8 m), and the receiver-tube emissivity had to be reduced to 0.2. A higher concentration ratio and lower emissivity increased the incident radiation on the receiver tube while reducing radiative heat losses. A reduction in the gas flow rate from 10 ft^3/min (0.0047 m^3/s) to 1 ft^3/min (0.00047 m^3/s) also increased the bulk catalyst temperature by reducing the enthalpic heat losses due to flow and heat of reaction. Table 1 summarizes the simulated impacts of different combinations of the gas flow rate, receiver emissivity, and concentration ratio on the bulk average catalyst temperature.

Table 1. Summary of parametric analyses of simulated impacts of gas flow rate, receiver emissivity, and geometric concentration ratio on bulk average catalyst temperature.

Run	Gas Flow Rate (cfm)*	Receiver Emissivity	Concentration Ratio**	Bulk Average Catalyst Temperature (°C)
1	1	0.9	~70	444
2	10	0.9	~70	353
3	1	0.2	~70	688
4	10	0.2	~70	556
5	1	0.9	~120	558
6	10	0.9	~120	497
7	**1**	**0.2**	~120	**876**
8	**10**	**0.2**	~120	**777**

*1 cfm = 0.000472 m^3/s

**Trough apertures of 5 m and 8.4 m yield geometric concentration ratios of ~70 and ~120, respectively, with a receiver tube diameter of 0.07 m.

Figure 4 shows the simulated temperature distributions along the length of the receiver tube and along a cut plane near the exit of the receiver tube for Run 8. The temperatures gradually increase toward the exit of the receiver as the flowing gas gets heated from the concentrated sunlight. The bottom of the receiver tube is hotter than at the top because of the incident radiation reflected from the parabolic collector below. This yields a convective flow pattern of air around the receiver tube, which also contributes to convective heat loss from the exterior of the tube to the ambient.

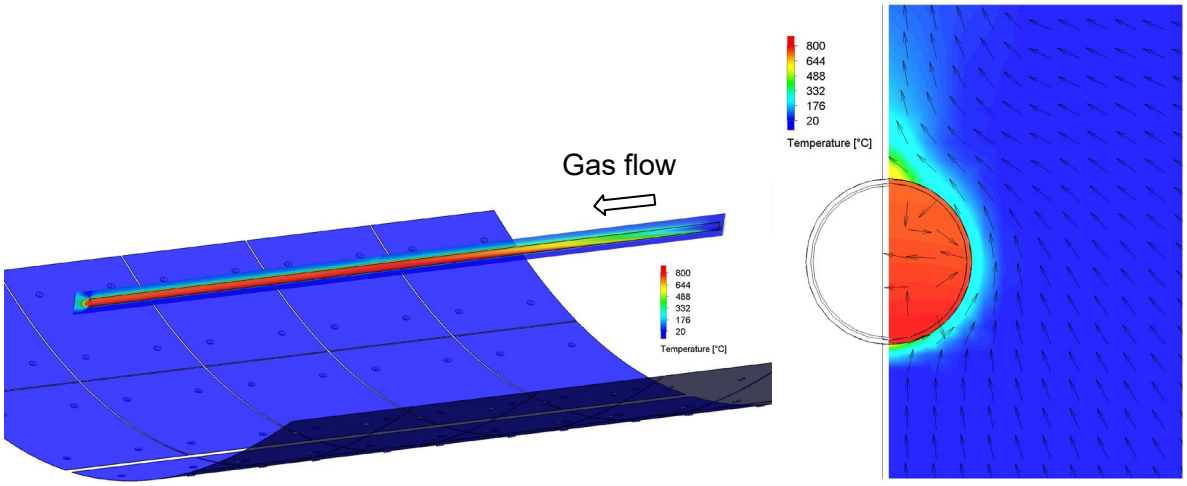

Figure 4. Left: Simulated temperature contours along a vertical cut plane through the receiver for Run 8. Right: Simulated temperature contours and gas flow vectors near the exit of the receiver tube.

Figure 5 shows the porous solid temperature of the preheat material and catalyst along the length of the receiver tube at the receiver centerline and near the bottom. At 4 m, when the inert porous material transitions to the catalyst, there is a sudden decrease in temperature near the bottom wall due to the heat of reaction enabled by the catalyst, which serves as a heat sink to the flowing gas in the model. After about a meter of distance into the catalyst, the temperature reaches a steady value, indicating an energy balance between the incident solar energy and heat losses.

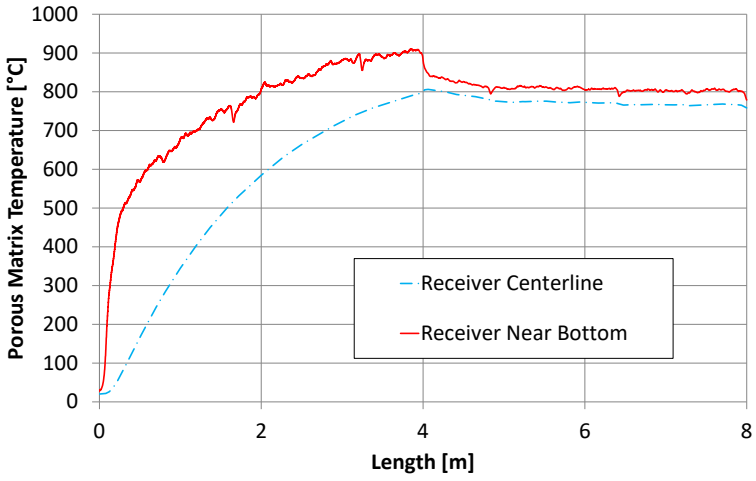

Figure 5. Porous matrix temperature as a function of flow length along the tube in Run 8.

Figure 6 shows the simulated pore velocities of the gas in the receiver tube for Run 8, which increase along the length of the tube. As the temperatures increase along the length of the tube, the temperature-dependent density of the flowing gas decreases. Therefore, the velocity of the gas increases to maintain the same bulk mass flow rate as its density decreases.

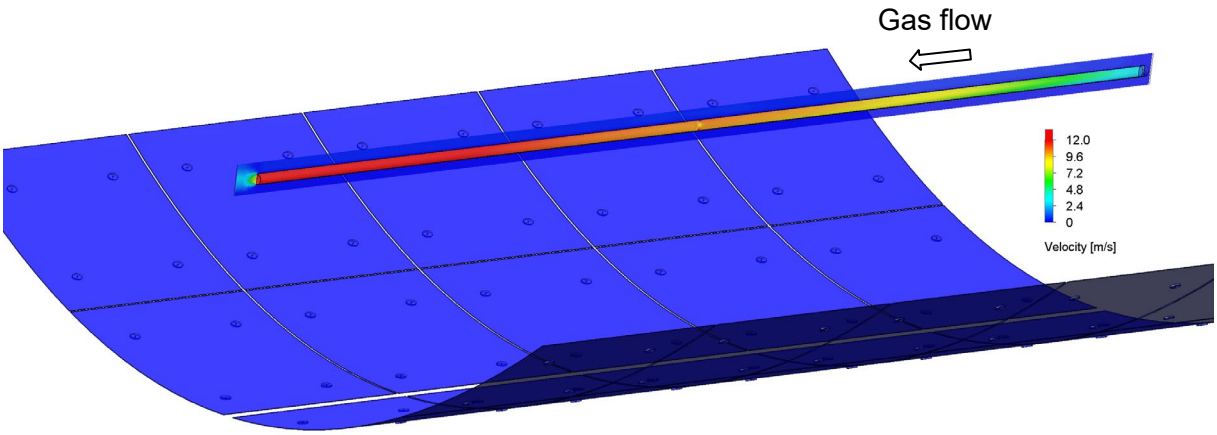

Figure 6. Simulated gas pore velocities in the receiver tube in Run 8.

Figure 7 shows the simulated pressure distribution in the receiver tube for Run 8. A simulated pressure drop of nearly 60 kPa was required to maintain the prescribed flow rate through the receiver tube. Parasitic power requirements for the blower need to be considered in future studies of the economics of the DRM system.

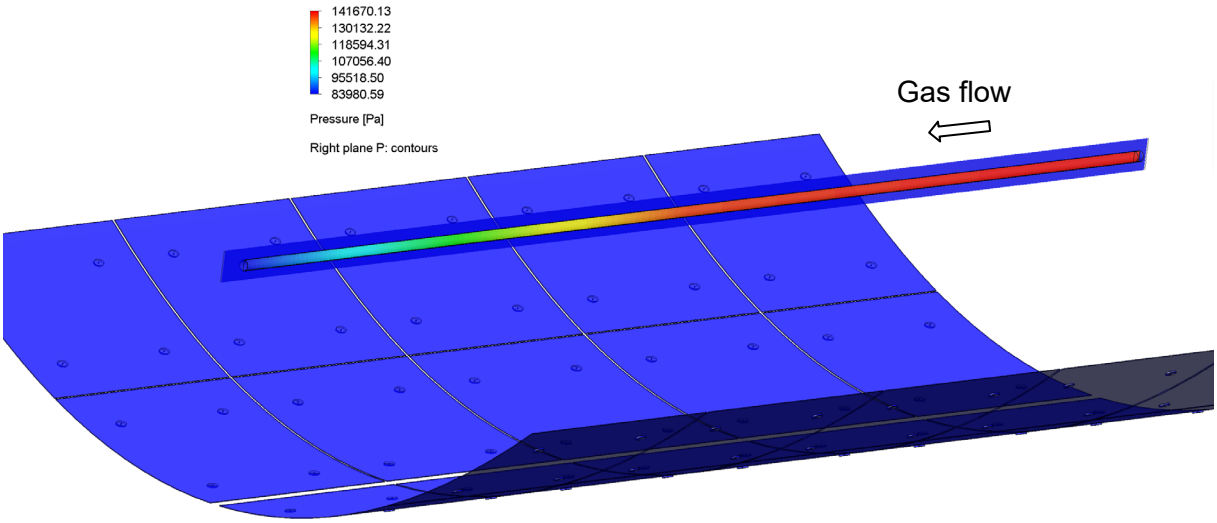

Figure 7. Simulated pressure distribution in the receiver tube in Run 8. The reference ambient pressure was assumed to be 84,000 Pa (Albuquerque, NM USA).

4 Conclusions

CFD simulations of CH_4 and CO_2 gas flow through a parabolic-trough receiver tube filled with porous material including a multi-cationic aluminate spinel catalyst were performed to evaluate configurations that could achieve the required 700 °C catalyst temperature to convert the feed gases to H_2 and CO. Results showed that increased geometric concentration ratios (from ~70 to ~120) and reduced receiver-tube emissivities (from 0.9 to 0.2) were required to achieve bulk

average catalyst temperatures of at least 700 °C. Lower gas flow rates (from 10 cfm (0.0047 m^3/s) to 1 cfm (0.00047 m^3/s)) also increased catalyst temperatures by reducing heat losses from the enthalpic heat losses of the flowing gas and the endothermic heat of reaction, which depends on the molar flow rate.

Future work should evaluate the technoeconomic trade-offs of larger trough apertures (5 m to ~8 m), the use of selective coatings and materials to reduce receiver-tube emissivities to ~0.2, and lower flow rates to achieve the required catalyst temperatures. Parasitic power requirements of the blower should also be considered. In addition, the current study assumed a fixed heat of reaction (heat sink), assuming that the feed gas of CH_4 and CO_2 was completely reacted within the prescribed length of the catalyst bed. Future studies should consider the kinetics of reaction and required length of the catalyst bed as a function of flow rate and other operating conditions.

Data availability statement

The CFD modeling in this study used thermophysical properties for fluids (air, methane) and solid materials provided in the commercial CFD code Solidworks Flow Simulation [7] and as cited in this paper.

Underlying and related material

The CFD code, Solidworks Flow Simulation [7], is commercially available. The model can be reproduced using the information provided in this paper.

Author contributions

Dr. Ho developed the design of the DRM trough system with preheat and performed the CFD simulations. Dr. Riley provided information regarding the catalyst and operating conditions.

Competing interests

The authors declare no competing interests.

Funding

Funding was provided through Sandia's Laboratory Directed Research and Development program (Project 224479).

Acknowledgement

Sandia National Laboratories is a multimission laboratory managed and operated by National Technology and Engineering Solutions of Sandia, LLC, a wholly owned subsidiary of Honeywell International, Inc., for the U.S. Department of Energy's National Nuclear Security Administration under contract DE-NA0003525. SAND2022-12652 C

References

1. United States Department of Energy, 2019, Natural Gas Flaring and Venting: State and Federal Regulatory Overview, Trends, and Impacts, Office of Oil and Natural Gas, Office of Fossil Energy, Washington, D.C.

2. Schulz, R., C. McGlade, and P. Zeniewski, 2021, Flaring Emissions, International Energy Agency,
3. Umukoro, G.E. and O.S. Ismail, *Modelling emissions from natural gas flaring.* Journal of King Saud University - Engineering Sciences, 2017. **29**(2): p. 178-182.
4. Agrafiotis, C., et al., *Solar thermal reforming of methane feedstocks for hydrogen and syngas production—A review.* Renewable and Sustainable Energy Reviews, 2014. **29**: p. 656-682.
5. Said, S.A.M., M. Waseeuddin, and D.S.A. Simakov, *A review on solar reforming systems.* Renewable and Sustainable Energy Reviews, 2016. **59**: p. 149-159.
6. Zhao, Q., et al., *Mid/low-temperature solar hydrogen generation via dry reforming of methane enhanced in a membrane reactor.* Energy Conversion and Management, 2021. **240**: p. 114254.
7. Dassault Systems, 2019, Technical Reference Solidworks Flow Simulation 2019,
8. Ho, C.K. and W. Gerstle, *Terrestrial Heat Repository for Months of Storage (THERMS): A Novel Radial Thermocline System*, in *ASME ES 2021 15th International Conference on Energy Sustainability*2021: Virtual
9. Wu, C.C. and G.J. Hwang, *Flow and heat transfer characteristics inside packed and fluidized beds.* Journal of Heat Transfer-Transactions of the ASME, 1998. **120**(3): p. 667-673.
10. Christian, J.M. and C.K. Ho, *Finite Element Modeling and Ray Tracing of Parabolic Trough Collectors for Evaluation of Optical Intercept Factors with Gravity Loading.* Proceedings of the ASME 5th International Conference on Energy Sustainability 2011, Pts a-C, 2012: p. 577-585.